Spatial integral projection models predict slow creosotebush encroachment between episodes of rapid expansion

Trevor Drees[*a,b], Brad M. Ochocki[b], Scott L. Collins[c], and Tom E.X. Miller[b]

[a]Department of Biology, Penn State University, State College, PA USA

[b]Program in Ecology and Evolutionary Biology, Department of BioSciences, Rice University, Houston, TX USA

[c]Department of Biology, University of New Mexico, Albuquerque, NM USA

November 12, 2020

[*]thd5066@psu.edu

Abstract

Encroachment[1] of shrubs into adjacent grasslands has become an increasingly reported phenomenon across the world, and such encroachment is either pulled forward by high population growth at the low-density encroachment front or pushed forward by higher-density areas behind the front. However, at sites such as Sevilleta National Wildlife Refuge in central New Mexico, little is known about whether encroachment is pushed or pulled, and the dynamics of encroachment are not well-understood. Here, long-term encroachment of creosotebush (Larrea tridentata), a native perennial shrub, stands in stark contrast with the stagnation in encroachment observed in recent decades. In order to better understand creosotebush encroachment at this site, we quantify it using a spatially structured population model where a wave of individuals travels at a speed governed by both dispersal and density-dependence. Results indicate that population growth rates generally increase with decreasing density, suggesting that encroachment is pulled by individuals at the low-density wave front, and the spatial population model predicts an encroachment rate of less than 2 cm per year. While the predicted rate of encroachment is consistent with observations over recent decades, it does not explain long-term creosotebush encroachment at the study site, suggesting that this process may occur in pulses when recruitment, seedling survival, or dispersal significantly exceed typical rates. Overall, our work demonstrates that individuals at low densities are likely the biggest contributors to creosotebush encroachment at this site, and that this encroachment is likely a process that occurs in large but infrequent bursts rather than at a steady pace.

Keywords

density-dependence, ecotones, woody encroachment, shrubs, integral projection model, grassland

---

[1] *I am not editing the abstract for now.*

Introduction

The encroachment of shrubs and other woody plants into adjacent grasslands has caused significant vegetation and landscape changes in ecosystems where this process takes place, and as such has become the focus of an increasing number of studies in recent years. This process of encroachment generally involves increases in number and/or density[2] of woody shrub-like plants in a given area (Van Auken, 2000), which can displace other species and alter abiotic aspects of the local ecosystem. Woody plant encroachment has been observed across many arid and semi-arid regions, such as the grasslands of the southwestern United States (Van Auken, 2000, 2009; Goslee et al., 2003; Gibbens et al., 2005) and southern South America (Parizek et al., 2002; Cabral et al., 2003), savannas of southern Africa (Trollope et al., 1989; Roques et al., 2001), and Asian steppes (Peng et al., 2013; Chen et al., 2015). Such encroachment may involve native or invasive plants and can adversely affect ecosystems in which it occurs, as the resulting increases in shrub biomass and density are considered to be strong drivers of ecosystem degradation and/or desertification (Schlesinger et al., 1990; Ravi et al., 2009) due to how these plants alter the distribution of soil resources (Schlesinger and Pilmanis, 1998; Knapp et al., 2008). Other adverse effects of encroachment include changes in ecosystem services (Reed et al., 2015; Kelleway et al., 2017), declines in biodiversity (Ratajczak et al., 2012; Sirami and Monadjem, 2012; Brandt et al., 2013), and economic losses in areas where the proliferation of shrubs adversely affects grazing land and pastoral production (Mugasi et al., 2000; Oba et al., 2000). [3]

The encroachment of woody plants into adjacent grasslands involves the movement of shrub-grass ecotones where a population of individuals is a gradient of conspecific density, and propagates as a wave across space and over time (Kot et al., 1996; Neubert

---

[2]*this description misses the spatial aspect*

[3]*I think it would be good for this first paragraph to introduce the idea of habitat ecotones, the need to understand whether these are stable, and how they may respond to global change drivers. You can then introduce woody encroachment as a specific and widespread type of ecotone.*

and Caswell, 2000; Wang et al., 2002; Pan and Lin, 2012). The movement of these waves is largely dependent upon two processes: local demography and dispersal of propagules. First, demographic processes affect how populations expand since survival, growth, reproduction, and recruitment rates in the parent plant ultimately affect the number of propagules produced and their fate after release, which is important because these propagules are the very basis for population growth. Second, movement is driven by the spatial dispersal of propagules produced by parent plants, and dispersal plays a role in where the new recruits that drive the wave's movement are likely to be found. The speed at which expansion waves move is highly dependent upon the shape of the dispersal kernel, or the probability distribution of dispersal distances, and is strongly influenced by the frequency of long-distance dispersal events at the tail of the distribution (Skarpaas and Shea, 2007). Additionally, both demography and dispersal are affected by population structure based on age, size, or life stage, which can strongly influence how waves move (Neubert and Caswell, 2000). For example, the reproductive aspect of demography in some plants is affected by age and size, as older individuals may be more likely to reproduce than younger individuals (Hanzawa and Kalisz, 1993) and larger individuals may reproduce more than smaller individuals (PICKERING, 1994; Smith et al., 2003). This means that within a population of plants, it is possible for the older or taller subset of the population to contribute disproportionately to the next generation. When it comes to dispersal, height influences dispersal via gravity or wind (Nathan et al., 2011) and the propagules of taller plants may travel further than those of their shorter counterparts, possibly making the taller individuals influential contributors to the spatial expansion a the population.

Given that expansion waves typically correspond to gradients of conspecific density, the effects of density dependence on demographic rates and population growth are important to consider. Conspecific density affects plants through intraspecific competition for resources: not only does density influence how plants survive, grow, and reproduce,

but it may also determine whether dispersed propagules germinate or are prevented from establishing. Since intraspecific competition governs the performance of individuals within the population, the location of the individuals most responsible for population wave movement is strongly tied to how demographic rates and population growth vary with changes in conspecific density. If population growth has a negative and monotonic relationship with density such that highest rates of population growth tend to be found at the lowest densities, then the invading wave is pulled forward by the plants at the low-density vanguard (Kot et al., 1996). However, if Allee effects result in reduced fitness at low densities[4], then the wave is instead pushed forward by the individuals behind the front edge (Kot et al., 1996; Taylor and Hastings, 2005; Sullivan et al., 2017). Such Allee effects can greatly limit population growth at the front of the wave, slowing[5] or halting its movement (Lewis and Kareiva, 1993; Veit and Lewis, 1996; Keitt et al., 2001).

[6]

In this study, we use data from an ecosystem in which woody encroachment occurs to link the encroachment process to ecological theory for invasion waves, with the goal of better understanding how demographic processes and dispersal drive this encroachment, and determining whether a particular instance of woody encroachment is pushed or pulled. The woody encroachment modelled here comes from study sites in the Chihuahuan Desert of the southwestern United States, where extensive documentation of shrub encroachment exists but little is known about the dispersal and demographic processes that govern it. In areas such as New Mexico, populations of the creosotebush (*Larrea tridentata*) have been expanding into nearby grasslands for approximately 150

---

[4]*I think this needs to be unpacked a bit more, explaining why fitness may be reduced at low density.*

[5]*I think it would help to have a more explicit statement that, all else equal, a pushed wave should be slower than a pulled wave – I think this is true but we should check and cite, obviously. See two nice references that I will email.*

[6]*I think there should be a new paragraph here that connects the pulled/pushed ideas to shrub encorachment. There is a lot of literature on woody plants being ecosystem engineers. While these are not typically called 'Allee effects', you can make the link that we might expect positive density dependence at the leading edge of woody ecotones, and this could slow or halt their expansion. I think this will be an important addition for building your story.*

years and have decreased the cover of grasses such as Bouteloua eriopoda (Gardner, 1951; Buffington and Herbel, 1965; Gibbens et al., 2005). This encroachment leads to ecotones marking a transition from dense shrubland with numerous dry patches to open grassland, with a transition zone in between where shrubs can often be found interspersed among their grassy competitors. Historically, long-term creosotebush encroachment into grasslands is believed to have been driven by a combination of factors including overgrazing, drought and variability in rainfall, and suppression of fire regimes Moreno-de las Heras et al. (2016). These shrubs are also thought to further facilitate their own encroachment through positive feedback (Grover and Musick, 1990; D'Odorico et al., 2012) by modifying various abiotic aspects of their local environment that could favour continued growth and dispersal[7], such as local climate (D'Odorico et al., 2010) and rates of soil erosion (Turnbull et al., 2010). Such positive feedback also occurs as herbaceous competitors are eliminated, reducing competition as well as the amount of flammable biomass used to fuel the fires that keep creosotebush growth in check (Van Auken, 2000). The existence of positive feedback mechanisms where creosotebush is present suggests that a lack of conspecifics at the low-density front of encroachment may depress population growth and be indicative of an Allee effect, though this has not yet been demonstrated.

While there is considerable interest in creosotebush encroachment, literature investigating the dispersal mechanisms and demographic processes that govern this process is extremely limited, and no previous studies have evaluated demography and dispersal to understand and predict creosotebush expansion dynamics. We have little understanding of how dispersal, density-dependent demography, and density-dependent population growth facilitate creosotebush encroachment, as well as a dearth of data regarding population dynamics at the vanguard of expanding creosotebush populations. Without better knowledge on all of these, it becomes rather difficult to model creosotebush encroachment, as doing so requires knowledge of the mechanisms occurring at these grass-shrub

---

[7] *Again, I would connect this back to Allee effects/pushed waves, since it suggests that seeds that recruit into high grass densities at the leading edge should suffer from lack of conspecifics.*

boundaries. Such gaps in knowledge make it difficult to make estimates of encroachment rates that extend beyond what can be gathered from vegetation surveys.

Our investigations are novel in the sense that they will be some of the first to apply a wave model of population expansion to ecotones of Larrea tridentata and its grassy competitors, using density-dependent demographic rates and recruitment to describe the dynamics of ecotone movement in this specific system. This research aims to fill the aforementioned knowledge gaps by not only collecting data on demographic rates and dispersal in Larrea tridentata, but by examining creosotebush encroachment in the framework of a wave model; by examining this system in such a way we can estimate the rate of creosotebush encroachment, and additionally determine whether this encroachment is pulled by the low-density wavefront pushed by high-density areas behind the wavefront. As such, we address the following questions: 1) What is the observed rate of creosotebush encroachment in recent past? 2) How do creosotebush size and conspecific density affect demographic rates such as growth and reproduction? 3) What does the dispersal kernel for this species look like and how far do propagules typically travel? 4) Using a wave model, what is the estimated rate of encroachment, and does it differ from the observed rate? and 5) Is the encroachment pulled by the individuals at the front of the wave or instead pushed by the individuals behind it? To answer these questions, we use a spatial integral projection model that combines dispersal data with demography data from surveys and transplant experiments.

Materials and methods

Study system

Paragraph about creosotebush at the SEV. [WIP] Creosotebush is a woody perennial native that is extremely drought-resistant and has a typical lifespan of # years. These shrubs are extremely efficient at absorbing water from the soil and tend to create large patches

7

of barren soil where nothing else can grow. Creosotebush reproduces both asexually and sexually. Shrubs can contain numerous small, yellow flowers that eventually give rise to highly pubescent seeds. Seeds are dispersed from the parent plant by gravity and wind, and can experience secondary dispersal by kangaroo rats. Here, we examine the encroachment of creosotebush at the Sevilleta National Wildlife Refuge in central New Mexico. This area receives approximately # of rainfall per yea andr consists of lowland shrub-grass ecotones as well as mountainous areas with juniper and pinon pine. While there is a history of creosotebush encroachment at the SEV, it seems to have stagnated over the past few decades; the reasons for this are largely unknown.

Encroachment re-surveys

We recorded shrub percent cover along two permanent 1000-m transects that spanned the shrub-grass ecotone, from high to low to near-zero shrub density. These surveys were conduced in summer 2001 and again in summer 2013 to document change in the spatial extent of shrub encroachment. At every 10 meters, shrub cover was recorded in nine cover classes (<1%, 1–4%, 5–10%, 10–25%, 25–33%, 33–50%, 50–75%, 75–95%, >95%). For analysis, we visually assessed midpoint values of these cover classes at each meter location for both transects and years.

Annual censuses

Demographic data collection

Collection of creosotebush demographic data occurred during the early summer of every year from 2013-2017, at the Sevilleta National Wildlife Refuge LTER site in central New Mexico. Four different sampling sites in the eastern part of the reserve were designated, with each of the sites containing 3 different transects. Lengths of these transects varied from 200 to 600 m, and no two sites had identical compositions of transect lengths. Transect length was determined by the strength of vegetation transition, as areas where

8

shrubland more quickly transitions to grassland do not need as long of a transect to capture the gradient of densities as a more gradual transition does. All transects were placed longitudinally along the shrubland-grassland ecotone so a full range of shrub densities could be captured; each transect spanned shrub-dense "core" areas as well as grasslands with few shrubs and the transition zones in between.

Only plants within a metre of the transect on either side were considered when determining baseline shrub densities. These densities were calculated using initial measurements from 2013 and were assumed to remain relatively static over the course of the study; each density was recorded as the weighted total amount of shrub volume per 5-m transect subsection. The per-shrub volume was calculated as that of an elliptic cone, as this was found to be the figure most closely matching the plant's morphology, using the formula $V_i = \pi lwh/3$ where l, w, and h are the maximum length, maximum width, and height, respectively. Maximum length and width were measured so that they were always perpendicular to each other, and height was measured from the base of the woody stem at the soil surface to the highest part of the shrub. All three of these dimensional measurements were mutually orthogonal and were inclusive only of living parts of the shrub; dead wood and non-foliated outer sections were not included in measurements. The total weighted density for the window was then expressed as the sum of log-transformed volumes of each individual shrub contained within. Such a weighted density was chosen because density of individuals alone can often fail to be a useful measurement in environments where large size differences between plants of the same species exist. Different-sized plants may vary greatly in their ability to extract resources from the environment around them and may thus differ greatly in their degree of competitiveness (Weiner, 1990; HARA, 1993). By using a weighted density in terms of shrub volume, we were able to account for the extra competitiveness of larger shrubs and thus have a more accurate measurement of conspecific presence that is more suitable for a study population containing significant heterogeneity in size.

A subset of the shrubs used to calculate the baseline densities were tagged, with each plant given a unique identifier that allowed it to be recognised based on sampling site, transect number, and location within 50-m and 5-m subsections. These tagged shrubs then had various demographic measurements recorded on an annual basis. Maximum width, length, and height on each shrub were measured in order to calculate conical volume, using the formula given earlier. Survival status of the shrubs was also recorded, with dead individuals being noted and excluded from measurements in subsequent years. Counts of flowers and fruits on each shrub were recorded as well. In instances where shrubs had large numbers of reproductive structures that would prove difficult to reliably count, estimates were made, with a more accurate count on a fraction of the shrub being extrapolated to the entire individual. The position of each shrub along the transect was noted to a resolution of 5 m so that it could be matched with the baseline density of its corresponding subsection. For shrubs in which a given 5-m subsection was not recorded, their position was estimated to the nearest 50 m; however, compared to the number of finer-resolution 5-m subsections, this occurred relatively infrequently. Establishment of recruits was also accounted for, with new recruits observed within the study area tagged and measured.

Demographic data analysis

Collected demography data were then examined to investigate how weighted density and shrub volume affected four different demographic variables: survival, probability of flowering (i.e. producing at least one flower or fruit), annual growth, and number of reproductive structures. Each of these demographic variables was fit to a different mixed-effects model through maximum likelihood. Both survival and probability of flowering were each fit to generalised linear mixed-effects models using a binomial response and a logit link function. Annual growth was defined as $\ln(V_{t+1}/V_t)$ where V_{t+1} and V_t are the shrub volumes in the current and previous years, respectively, and was then fit to a linear

10

mixed-effects model. The number of reproductive structures was defined as the natural logarithm of the sum of fruits and flowers on the entire shrub and was fit to a linear mixed-effects model as well. To construct these models, all of the equations listed in Table 1 were first fit to each of the four demographic variables, with each equation using volume and standardised density as predictors while also treating the unique transect in which each shrub was located as a random effect. After these equations were fit to the data, all eight equations for each demographic variable were ranked based on their value of the Akaike information criterion (AIC) and weighted based on their quality so that better-fitting models had a higher weight. Then, coefficients of the same type were averaged between all eight models for each demographic variable using a weighted mean corresponding to model quality in order to generate an average model. All four average models have the general form

$$R = \beta_1 v + \beta_2 d + \beta_3 d^2 + \beta_4 vd + \beta_5 vd^2 + \epsilon \tag{1}$$

where R is the response variable, v and d are the volume and density, ϵ is a random transect effect, and β is the coefficient for each type of term.

The effect of density dependence on the probability of recruitment from seeds was also modelled. For every year, the sum of seeds produced the prior year was calculated for each 5-m subsection, and then probability of recruitment was calculated as the number of recruits observed in each 5-m subsection divided by that number of seeds. For any subsection in which seeds were not found, a count of seeds was estimated based on the number of seeds in a subsection of similar weighted density; this was done to avoid creating any undefined values of recruitment probability. Both linear and quadratic models using only weighted density as a predictor were fit to the distribution of recruitment probabilities, though the linear model was ultimately used because it had a higher AIC value.

Transplant experiment

Transplant data collection

Transplant data analysis

Dispersal modelling

Dispersal kernels were calculated using the WALD, or Wald analytical long-distance dispersal, model that uses a mechanistic approach to predict dispersal patterns of plant propagules by wind. The WALD model, which is largely based in fluid dynamics, can serve as a good approximation of empirically-determined dispersal kernels (Katul et al., 2005; Skarpaas and Shea, 2007) and may be used when empirical dispersal data is not readily available. Under the assumptions that wind turbulence is low, wind flow is vertically homogenous, and terminal velocity is achieved immediately upon seed release, the WALD model simplifies a Lagrangian stochastic model to create a dispersal kernel that estimates the likelihood a propagule will travel a given distance (Katul et al., 2005). This dispersal kernel takes the form of the inverse Gaussian distribution

$$p(r) = \left(\frac{\lambda'}{2\pi r^3} \right)^{\frac{1}{2}} \exp \left[-\frac{\lambda'(r - \mu')^2}{2\mu'^2 r} \right] \tag{2}$$

that is a slight adaptation from equation 5b in Katul et al. (2005), using r to denote dispersal distance. Here, λ' is the location parameter and μ' is the scale parameter, which depend on environmental and plant-specific properties of the study system. The location and scale parameters are defined as $\lambda' = (H/\sigma)^2$ and $\mu' = HU/F$; these are functions of the height H of seed release, wind speed U at seed release height, seed terminal velocity F, and the turbulent flow parameter σ that depends on both wind speed and local vegetation roughness.

In order to create the dispersal kernel, we first take the wind speeds at measurement height z_m and correct them to find wind speed U for any height H by using the

logarithmic wind profile

$$U = \frac{1}{H} \int_{d+z_0}^{H} \frac{u^*}{K} \log\left(\frac{z-d}{z_0}\right) dz \tag{3}$$

given in Bullock et al. (2012) equation 6, with the notation slightly modified. Here, z is the height above the ground, K is the von Karman constant, and u^* is the friction velocity. The zero-plane displacement d and roughness length z_0 are surface roughness parameters that, for a grass canopy height h above the ground, are approximated by $d \approx 0.7h$ and $z_0 \approx 0.1h$. These estimates are from Raupach (1994) for a canopy area index $\Lambda = 1$ in which the sum of grass canopy elements is equal to the unit area being measured. A 0.15 m grass height at the study site gives $d = 0.105$ and z_0, which are suitable approximations for grassland (Wiernga, 1993). Calculations of u^* were done using equation A2 from Skarpaas and Shea (2007), in which

$$u^* = KU_m \left[\log\left(\frac{z_m - d}{z_0}\right)\right]^{-1} \tag{4}$$

and U_m is the mean wind velocity at the measurement height z_m. Values for the turbulent flow parameter σ were then calculated using the estimate made by Skarpaas and Shea (2007) in their equation A4, where

$$\sigma = 2A_w^2 \sqrt{\frac{K(z-d)u^*}{C_0 U}} \tag{5}$$

and C_0 is the Kolmogorov constant. A_w is a constant that relates vertical turbulence to friction velocity and is approximately equal to 1.3 under the assumptions of above-canopy flow made by Skarpaas and Shea (2007), based off calculations from Hsieh and Katul (1997). In addition, the assumption that $z = H$ was made in order to make the calculation of σ more feasible.

The values from the previous three equations give us the necessary information to

13

calculate μ' and λ', thus allowing us to create the WALD distribution $p(r)$. However, the base WALD model does not take into account variation in wind speeds or seed terminal velocities, which limits its applicability in systems where such variation is present. In order to account for this variation, we integrate the WALD model over distributions these two variables using the same method as Skarpaas and Shea (2007). The WALD model assumes seed release from a single point source, though, which is not realistic for a shrub; because seeds are released across the entire height of the shrub rather than from a point source, $p(r)$ was also integrated across the uniform distribution from the grass canopy height to the shrub height. Thus, under the assumptions that the height at which a seed is located does not affect its probability of being released and that seeds are evenly distributed throughout the shrub, this gives the dispersal kernel $K(r)$, where

$$K(r) = \iiint p(F)p(U)p(z)p(r)\,dF\,dU\,dz \tag{6}$$

and $p(F)$ and $p(U)$ are the PDFs of the terminal velocity F and wind speed U, respectively, and $p(z)$ is the uniform distribution from h to H.

The distribution $p(F)$ in the integral above was constructed using experimentally determined seed terminal velocities. This was done by using a high-speed camera and motion tracking software to determine position as a function of time, and then using the Levenberg-Marquardt algorithm to solve a quadratic-drag equation of motion for F. Before seeds were released, they were dried and then dyed with yellow fluorescent powder, and then put against a black background to improve visibility and make tracking easier. While the powder added mass to the seeds, this added mass only yielded an approximately 2.5% increase and was thus negligible, likely having little effect on their terminal velocities. Measurements were conducted for 48 seeds that were randomly chosen from a seed pool derived from different plants, and then an empirical PDF of terminal velocities was constructed using the data. Constructing $p(U)$ involved creating an empirical PDF

of hourly wind speeds at Five Points, the site closest to the 12 transects being used, that were obtained from meteorological data collected at the Sevilleta National Wildlife Refuge from 1988 to 2010. We did not weight $p(U)$ and assumed that the probability seed release from the shrub is the same regardless of wind speed.

Spatial integral projection model

Given that the shrub population at this site is approximately homogeneous perpendicular to the direction of encroachment, expansion is modelled as a wave moving in one dimension. A spatial integral projection model (SIPM) is used to estimate the speed at which encroachment occurs; such a model incorporates the effects of variation in traits like plant size that stage-structured models, such as those described in Neubert and Caswell (2000), do not capture. According to Jongejans et al. (2011), a general SIPM can be formulated as

$$\mathbf{n}(x_2, z_2, t+1) = \iint \tilde{K}(x_2, x_1, z_2, z_1)\mathbf{n}(x_1, z_1, t)\, dx_1\, dz_1 \tag{7}$$

where x_1 and x_2 are locations of individuals of a particular size before and after one unit of time, and z_1 and z_2 are the respective sizes. The vector $\mathbf{n}$ indicates the population density of each size, and $\tilde{K}$ is a kernel that combines dispersal with demography. Though this SIPM represents a continuous spectrum of shrub sizes and densities, it was implemented by discretising the above integral with a 200 x 200 matrix, as this makes calculations significantly more tractable.

Movement of the wave is determined by the components of the combined dispersal/demography kernel $\tilde{K}$, which is of the same form as that used in Jonjegans et al. (2011). Here,

$$\tilde{K}(x_2, x_1, z_2, z_1) = K(x_2 - x_1)Q(z_2 - z_1) + \delta(x_2 - x_1)G(z_2 - z_1) \tag{8}$$

and K is the dispersal kernel, Q a reproduction function, G a growth function, and δ the Dirac delta function. G is derived from the model for annual growth ratio, and Q is derived from the reproductive structures model as well as other factors including number of seeds per reproductive structure, probability of recruitment from seed, and recruit size. Both G and Q give the probability of transition between sizes; in the case of G, this is the probability of growing from one specific size to another, and in the case of Q the probability that an individual of a specific size produces a recruit of a specific size. The product of K and Q represents the production and dispersal of motile propagules, while the product of G and δ represents the growth of sessile individuals.

Given growth function G and the reproduction function Q, the speed of the moving wave can be calculated as

$$c^* = \min_{s>0} \left[\frac{1}{s} \ln(\rho_s) \right] \tag{9}$$

where s is the wave shape parameter and ρ_s is the dominant eigenvalue of the kernel $\mathbf{H_S}$ (Jongejans et al., 2011). This estimate for the wavespeed is valid under the assumption that population growth decreases monotonically as conspecific density increases, with the highest rates of growth occurring at the lowest population densities (Lewis et al., 2006). The kernel $\mathbf{H_S}$ is defined as

$$\mathbf{H_S} = M(s)Q(z_2 - z_1) + G(z_2 - z_1) \tag{10}$$

where $M(s)$ is the moment-generating function of the dispersal kernel (Jongejans et al., 2011). For one-dimensional dispersal, this moment-generating function can be estimated as

$$M(s) = \frac{1}{N} \sum_{i=1}^{n} I_0(sr_i) \tag{11}$$

where r is the dispersal distance for each observation, and I_0 is the modified Bessel function of the first kind and zeroth order (Skarpaas and Shea, 2007). In order to obtain

16

370 M, numerous dispersal distances were simulated from the dispersal kernel $K(r)$ described

371 in the previous section, with over 2000 replications for each shrub height increment of 1

372 cm. This was performed over the range from the lowest possible dispersal height to the

373 maximum shrub height. Once $M(s)$ was obtained for dispersal at each shrub height, $\mathbf{H_S}$

374 and c^* were calculated for each value of s; this was done for values of s ranging from 0

375 to 2, as it is this range in which c^* occurs.

Results

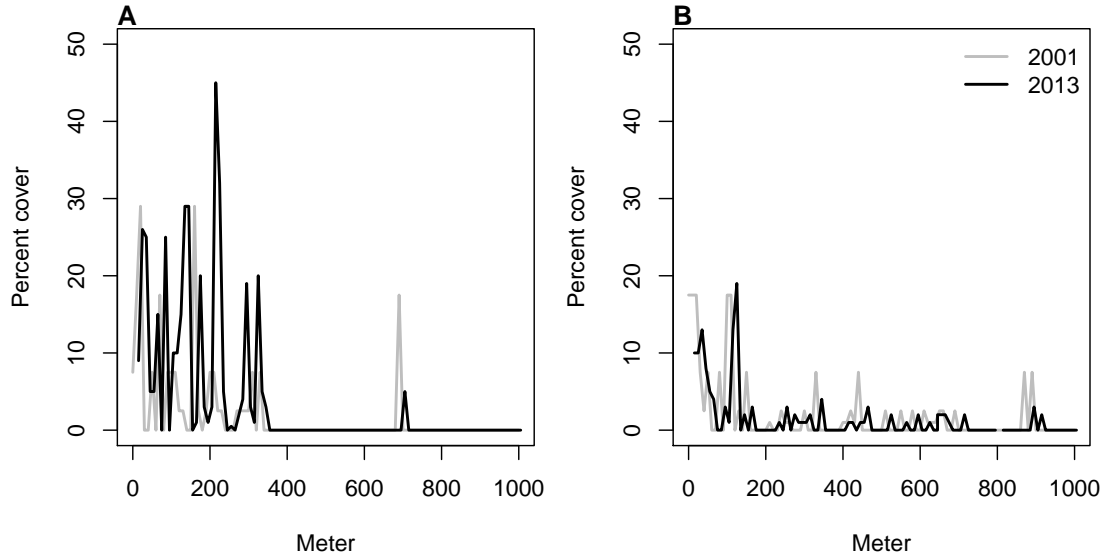## Encroachment re-surveys

Figure 1.

Figure 1: Re-surveys of shrub cover along two permanent trasects (A,B) surveyed in 2001 and 2013.

379 The speed of encroachment at the study site as estimated by the SIPM is rather

380 slow; as can be seen in Figure 2, the low-density wavefront moves at approximately

381 0.5 cm/yr under normal conditions and at 1 cm/yr under the best seedling survival

382 conditions observed in the dataset. These improved conditions were observed due to

above-average rainfall that occurred after greenhouse-grown seedlings were transplanted to the site. Population growth in this low-density region of the moving wave is also low, with a geometric growth rate of $\lambda \approx 1.006$ and even lower rates of growth the higher-density regions behind; in the higher-survival scenario the maximum rate increases to $\lambda \approx 1.013$, with growth still decreasing as density increases. For both scenarios, the decrease in population growth rate with increasing density was monotonic across the range of observed standardised densities, as is shown in Figure 2. This suggests that an Allee effect is likely not present in this population, as the highest rate of population growth is found at the lowest density vanguard of the encroaching population. Thus, the conditions necessary for equation 9 to be valid are satisfied, and these wavespeeds are applicable for a pulled-wave scenario in which no Allee effects are present.
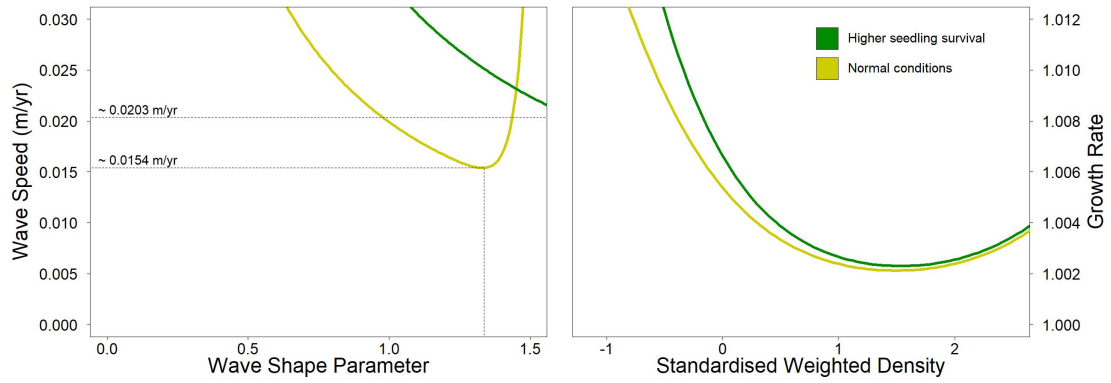

Figure 2: Estimated encroachment wave speeds (left) and geometric rates of population growth (right) for higher post-rainfall seedling survival and normal conditions.

As the speed of encroachment is quite limited, so is the extent of wind dispersal. Long distance dispersal events, while more common for taller shrubs than their shorter counterparts, are still uncommon overall. For the tallest shrub height of 1.98 m, only 0.32% of propagules exceed a dispersal distance of 5 m, and 0.02% exceed 10 m. At 1 m, or approximately half the tallest shrub height, long distance dispersal is even less likely, with 0.0046% of propagules exceeding a dispersal distance of 5 m and 0.0009%

exceeding 10 m. Given that the median shrub height is only 0.64 m, the occurrence of long-distance wind dispersal in most of the shrub population is highly improbable, and the few instances in which it occurs will only be limited to the tallest shrubs. Thus, as Figure 3 demonstrates, shorter dispersal distances dominate; even for the tallest shrub, 81% of seeds fall within only a metre of the plant, and this percentage increases as shrub height decreases. Dispersal kernels have their highest probability density at dispersal distances between 2 and 8 cm from the shrub; here, as shrub height increases, the most probable dispersal distance slightly increases while maximum probability density decreases. Regardless of the shrub height, most dispersal will occur very close to the plant, though increases in shrub height dramatically increase the likelihood of dispersal at longer distances. It is clear that the shape of the height-dependent dispersal kernel $K(r)$ varies greatly among the shrub population given the large range of shrub heights observed; shrubs at lower heights have more slender kernels with most of the seeds dispersing closer to the plant, while taller shrubs have kernels with much fatter tails and are more capable of longer-distance dispersal.
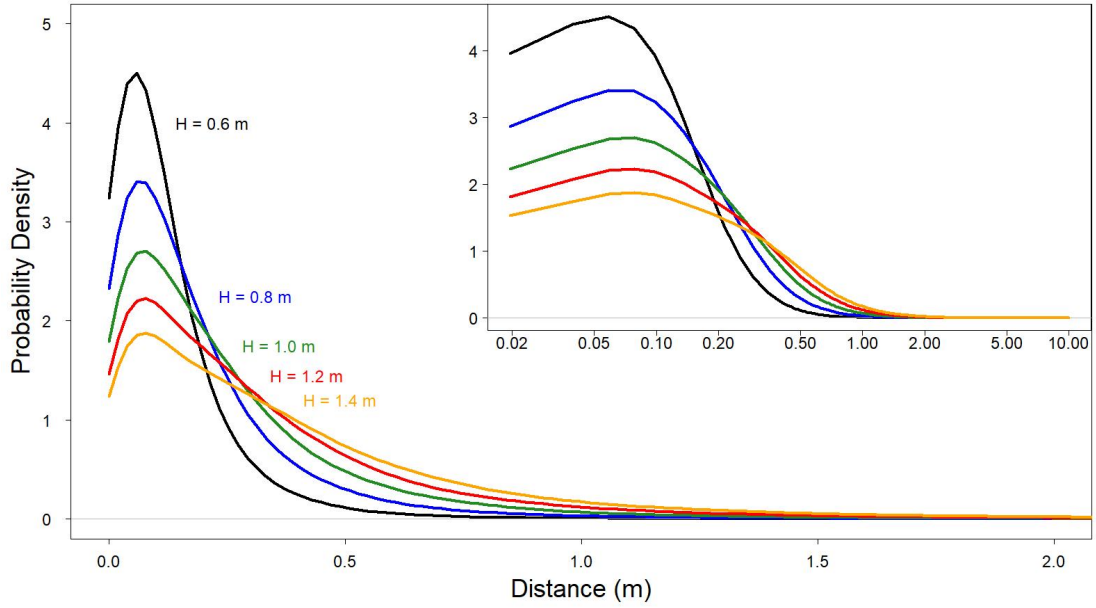
Figure 3: Dispersal kernels, with each colour representing a selected shrub height. The inset plot is the same as the large plot, though with a logarithmic x-axis to more easily show differences in dispersal probability at smaller distances.

Density and size dependence are evident in all 4 of the demographic rates, with coefficients for each model displayed in Table 2. For growth, reproduction, and survival, density dependence is mostly negative and monotonic; this is not the case for probability of flowering, where shrub size seems to be more important than the effects of density alone and suggests that larger shrubs have a higher probability of flowering than their smaller counterparts. This, along with size and density dependence in growth and reproduction, is shown in Figure 4. Size dependence is positive for reproduction, as would be expected since larger plants typically produce more flowers and fruits. However, annual growth decreases as size increases; this could be in part due to the annual growth in this study being quantified as a proportion relative to the shrub's initial size. While larger shrubs may produce more plant material over a year in terms of absolute volume, smaller shrubs produce less but can still have higher annual growth in terms of the percentage of volume

20

added relative to their initial volume. When compared to density, shrub size is a much stronger predictor of survival, with significant differences in mortality rates depending on shrub size. For small shrubs, mortality is exceptionally high, and increases in volume for these shrubs only slightly increase the likelihood of survival. However, after shrubs reach a logarithmic volume of approximately 7.3, they are almost guaranteed to survive, with survival rates near 100% persisting regardless of any further size increases. Interestingly, though most recruits were found at lower densities, the probability of recruitment from seed displays positive density dependence; the probability of recruitment was still very low, though, with a baseline rate of approximately 2 recruits per 10,000 seeds.
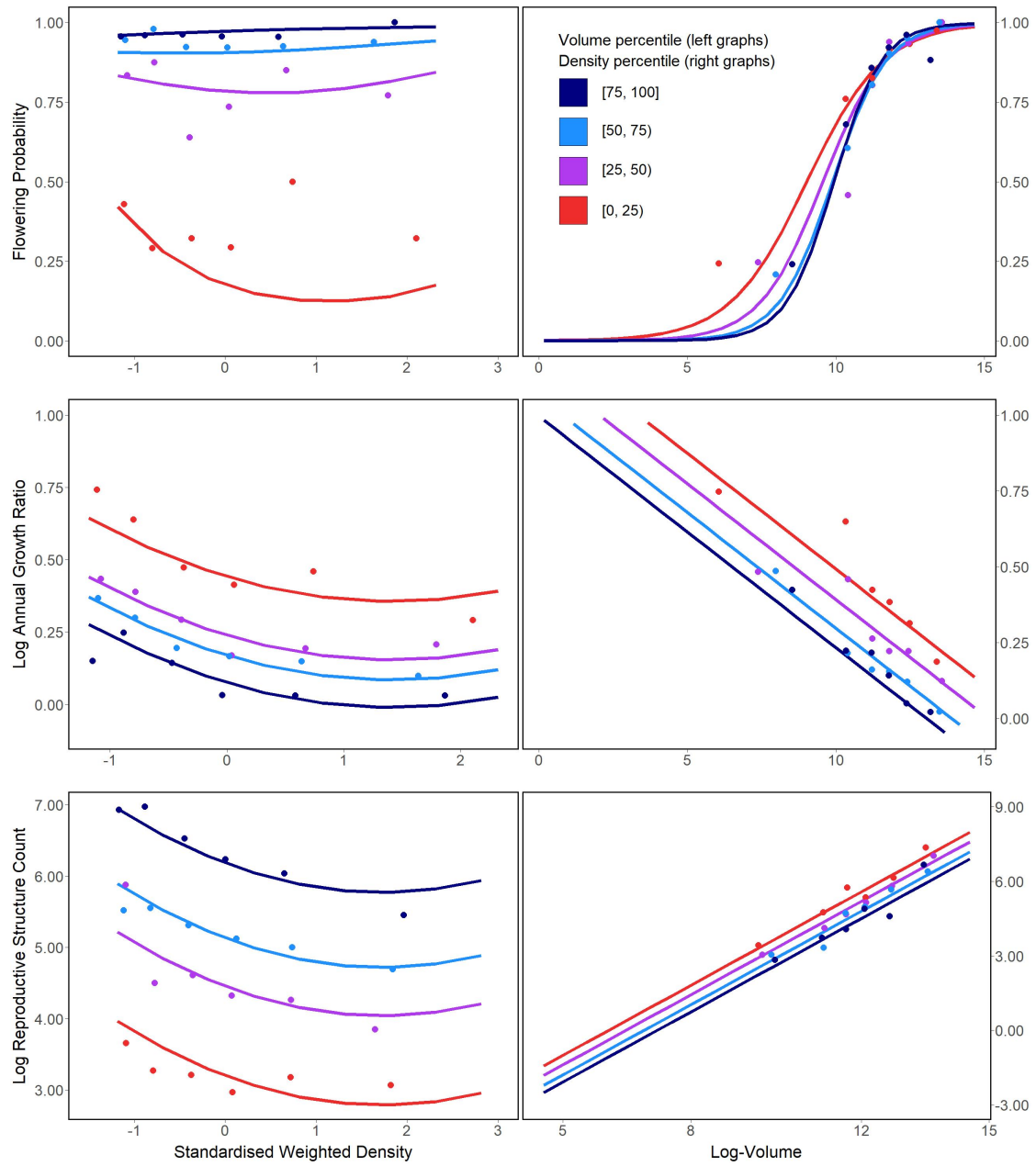
Figure 4: Flowering probability (top row), log annual growth ratio (centre row), and log reproductive structure count (bottom row) at all four sampling sites. In the left column of graphs, the three response variables are shown as a function of density for each of four volume quartiles, with each quartile containing six density bins; in the right column, the opposite occurs, with response variables shown as functions of four volume quartiles that each contain six density bins. Graphs quantifying the number of reproductive structures include data only on plants that flowered.

Discussion

The slow movement of the encroaching creosotebush wave at the Sevilleta LTER site can likely be contributed to a combination of three factors: short dispersal distances with extremely limited long-distance dispersal events, very low probability of recruitment from seed, and high seedling mortality. These three barriers, when combined, form a formidable challenge to the establishment of new shrubs at the low-density front of the wave. First, a seed must travel far enough to avoid competition with the parent shrub, which is unlikely given the dispersal kernels shown in Figure 2. Even if the seed manages to be dispersed this far, its chances of becoming a seedling are low. Caching and consumption by seed-eaters such as a variety of seed-harvesting ants (Whitford, 1978; Whitford et al., 1980; Lei, 1999) and the kangaroo rat Dipodomys merriami (Chew and Chew, 1970) decreases the amount of seeds available for germination. However, reduction in germination caused by destruction of seeds may be partly mitigated by the more favourable germination conditions that these seeds can experience when cached underground (Chew and Chew, 1970). Many of the remaining seeds will still fail to germinate, and in the unlikely event that germination does occur, seedlings will likely die given the high rates of mortality observed in smaller shrubs. Such high rates of creosotebush seedling mortality have been observed in other studies as well (Boyd and Brum, 1983; Bowers et al., 2004), probably due to a combination of herbivory, competition, and abiotic stresses.

However, as low as they are, the wavespeed estimates given in this paper are still conservative estimates for reasons mostly related to dispersal. First, it is important to note that the dispersal kernels used here, while they account for variation in factors such as wind speed and terminal velocity, may underestimate the distances that shrub propagules travel. Because the WALD model assumes that terminal velocity is reached immediately upon seed release, seeds in the estimate thus take a shorter time to fall

23

and have less time to be transported by wind, and the true frequency of long-distance dispersal events may thus be greater than what is estimated here. Second, dispersal at the study site could occur through additional mechanisms other than wind. For example, secondary dispersal through runoff from significant rainfall events can transport seeds (Thompson et al., 2014), and given that long-distance dispersal by bird and subsequent species divergence is thought to be responsible for creosotebush being in North America in the first place (Wells and Hunziker, 1976), short-distance dispersal by other animals at the study site likely occurs. As mentioned above, seeds are transported by seed-harvesting ants and granivorous mammals, where they are often stored in caches that can be appreciable distances from the parent shrubs. Whether transportation occurs via ant or rodent, creosotebush seeds can be moved significantly further than wind alone can, though many of these seeds are eventually consumed.

Despite the more conservative estimates our model yields, the estimated rate of dispersal in creosotebush populations at the Sevilleta National Wildlife Refuge is consistent with observations from the past 50-60 years, as creosotebush expansion during this time has been minimal (Moreno-de las Heras et al., 2016). However, it cannot explain the long-term increases in creosotebush cover at the study site, as total encroachment over the past 150 years is much greater than what would be expected given the encroachment rates derived by our models. Such a discrepancy is likely due to much of the expansion occurring in an episodic fashion, with short times during which rapid encroachment occurs due to favourable environmental conditions. This could be due in part to seedling recruitment, which is a factor that strongly limits creosotebush expansion, being rare and episodic. For example, Allen et al. (2008) estimate that a major recruitment event occurred at this site in the 1950s, which is supported by photographic evidence from Milne et al. (2003) of a drought-driven expansion during this time. Moreno-de las Heras et al. (2016) estimate that after this expansion, several smaller creosotebush recruitment events occurred in decadal episodes. However, such events can be highly localised and

24

may not necessarily occur at the low-density front of encroachment, which could explain how these recruitment events can still coexist with lack of encroachment in the recent past.

Overall, our observations and model highlight three aspects of creosotebush encroachment that should be the focus of future studies seeking to obtain better estimates of encroachment rates. First, negative density dependence in survival, growth, and reproduction is demonstrated, along with size dependence. The clear dependence on size and conspecific density suggests that they both should be considered when estimating creosotebush expansion and quantifying the demographic variation that contributes to it. Second, wind dispersal in these shrubs is quite limited; though the dispersal kernels seen here are typical in the sense that they are characterised by high near-plant dispersal and exceptionally low long-distance dispersal, the scale across which such dispersal occurs is small, with most seeds landing within only 1 m of the shrub. Wind dispersal alone may be an underestimate of the true amount of dispersal occurring, and future work should seek to incorporate the effects of dispersal by runoff and animals so that a more representative model of total dispersal can be obtained. Finally, encroachment is slow or even stagnates, but only most of the time. Though our encroachment speed estimates are representative of creosotebush populations for most years, the significant expansion seen over larger time scales suggests that there is episodic expansion in other years; while our model is consistent with the recent stagnation in creosotebush encroachment at the Sevilleta LTER site, a model that also includes interannual variability in factors such as survival and recruitment would be able to better account for instances of episodic population expansion that are characteristic of this location.

Acknowledgements

Author contributions

Data accessibility

References

Allen, A., W. Pockman, C. Restrepo, and B. Milne. 2008. Allometry, growth and population regulation of the desert shrub Larrea tridentata. Functional Ecology pages 197–204.

Bowers, J. E., R. M. Turner, and T. L. Burgess. 2004. Temporal and spatial patterns in emergence and early survival of perennial plants in the Sonoran Desert. Plant Ecology **172**:107–119.

Boyd, R. S., and G. D. Brum. 1983. Postdispersal reproductive biology of a Mojave Desert population of Larrea tridentata (Zygophyllaceae). American Midland Naturalist pages 25–36.

Brandt, J. S., M. A. Haynes, T. Kuemmerle, D. M. Waller, and V. C. Radeloff. 2013. Regime shift on the roof of the world: Alpine meadows converting to shrublands in the southern Himalayas. Biological Conservation **158**:116–127.

Buffington, L. C., and C. H. Herbel. 1965. Vegetational changes on a semidesert grassland range from 1858 to 1963. Ecological monographs **35**:139–164.

Bullock, J. M., S. M. White, C. Prudhomme, C. Tansey, R. Perea, and D. A. Hooftman. 2012. Modelling spread of British wind-dispersed plants under future wind speeds in a changing climate. Journal of Ecology **100**:104–115.

26

Cabral, A., J. De Miguel, A. Rescia, M. Schmitz, and F. Pineda. 2003. Shrub encroachment in Argentinean savannas. Journal of Vegetation Science **14**:145–152.

Chen, L., H. Li, P. Zhang, X. Zhao, L. Zhou, T. Liu, H. Hu, Y. Bai, H. Shen, and J. Fang. 2015. Climate and native grassland vegetation as drivers of the community structures of shrub-encroached grasslands in Inner Mongolia, China. Landscape Ecology **30**:1627–1641.

Chew, R. M., and A. E. Chew. 1970. Energy relationships of the mammals of a desert shrub (Larrea tridentata) community. Ecological Monographs pages 2–21.

D'Odorico, P., J. D. Fuentes, W. T. Pockman, S. L. Collins, Y. He, J. S. Medeiros, S. DeWekker, and M. E. Litvak. 2010. Positive feedback between microclimate and shrub encroachment in the northern Chihuahuan desert. Ecosphere **1**:1–11.

D'Odorico, P., G. S. Okin, and B. T. Bestelmeyer. 2012. A synthetic review of feedbacks and drivers of shrub encroachment in arid grasslands. Ecohydrology **5**:520–530.

Gardner, J. L. 1951. Vegetation of the creosotebush area of the Rio Grande Valley in New Mexico. Ecological Monographs **21**:379–403.

Gibbens, R., R. McNeely, K. Havstad, R. Beck, and B. Nolen. 2005. Vegetation changes in the Jornada Basin from 1858 to 1998. Journal of Arid Environments **61**:651–668.

Goslee, S., K. Havstad, D. Peters, A. Rango, and W. Schlesinger. 2003. High-resolution images reveal rate and pattern of shrub encroachment over six decades in New Mexico, USA. Journal of Arid Environments **54**:755–767.

Grover, H. D., and H. B. Musick. 1990. Shrubland encroachment in southern New Mexico, USA: an analysis of desertification processes in the American Southwest. Climatic change **17**:305–330.

27

Hanzawa, F. M., and S. Kalisz. 1993. The relationship between age, size, and reproduction in Trillium grandiflorum (Liliaceae). American Journal of Botany **80**:405–410.

HARA, T. 1993. Mode of competition and size-structure dynamics in plant communities. Plant Species Biology **8**:75–84.

Hsieh, C.-I., and G. G. Katul. 1997. Dissipation methods, Taylor's hypothesis, and stability correction functions in the atmospheric surface layer. Journal of Geophysical Research: Atmospheres **102**:16391–16405.

Jongejans, E., K. Shea, O. Skarpaas, D. Kelly, and S. P. Ellner. 2011. Importance of individual and environmental variation for invasive species spread: a spatial integral projection model. Ecology **92**:86–97.

Katul, G., A. Porporato, R. Nathan, M. Siqueira, M. Soons, D. Poggi, H. Horn, and S. A. Levin. 2005. Mechanistic analytical models for long-distance seed dispersal by wind. The American Naturalist **166**:368–381.

Keitt, T. H., M. A. Lewis, and R. D. Holt. 2001. Allee effects, invasion pinning, and species' borders. The American Naturalist **157**:203–216.

Kelleway, J. J., K. Cavanaugh, K. Rogers, I. C. Feller, E. Ens, C. Doughty, and N. Saintilan. 2017. Review of the ecosystem service implications of mangrove encroachment into salt marshes. Global Change Biology **23**:3967–3983.

Knapp, A. K., J. M. Briggs, S. L. Collins, S. R. Archer, M. S. BRET-HARTE, B. E. Ewers, D. P. Peters, D. R. Young, G. R. Shaver, E. Pendall, et al. 2008. Shrub encroachment in North American grasslands: shifts in growth form dominance rapidly alters control of ecosystem carbon inputs. Global Change Biology **14**:615–623.

Kot, M., M. A. Lewis, and P. van den Driessche. 1996. Dispersal data and the spread of invading organisms. Ecology **77**:2027–2042.

580 Lei, S. A. 1999. Ecological impacts of Pogonomyrmex on woody vegetation of a Larrea-
581 Ambrosia shrubland. The Great Basin Naturalist pages 281–284.

582 Lewis, M., and P. Kareiva. 1993. Allee dynamics and the spread of invading organisms.
583 Theoretical Population Biology **43**:141–158.

584 Lewis, M. A., M. G. Neubert, H. Caswell, J. S. Clark, and K. Shea, 2006. A guide
585 to calculating discrete-time invasion rates from data. Pages 169–192 *in* Conceptual
586 ecology and invasion biology: reciprocal approaches to nature. Springer.

587 Milne, B. T., D. I. Moore, J. L. Betancourt, J. A. Parks, T. W. Swetnam, R. R. Par-
588 menter, and W. T. Pockman. 2003. Multidecadal drought cycles in south-central New
589 Mexico: Patterns and consequences. Oxford University Press: New York, NY.

590 Moreno-de las Heras, M., L. Turnbull, and J. Wainwright. 2016. Seed-bank structure
591 and plant-recruitment conditions regulate the dynamics of a grassland-shrubland Chi-
592 huahuan ecotone. Ecology **97**:2303–2318.

593 Mugasi, S., E. Sabiiti, and B. Tayebwa. 2000. The economic implications of bush
594 encroachment on livestock farming in rangelands of Uganda. African Journal of Range
595 and Forage Science **17**:64–69.

596 Nathan, R., G. G. Katul, G. Bohrer, A. Kuparinen, M. B. Soons, S. E. Thompson,
597 A. Trakhtenbrot, and H. S. Horn. 2011. Mechanistic models of seed dispersal by wind.
598 Theoretical Ecology **4**:113–132.

599 Neubert, M. G., and H. Caswell. 2000. Demography and dispersal: calculation and
600 sensitivity analysis of invasion speed for structured populations. Ecology **81**:1613–
601 1628.

602 Oba, G., E. Post, P. Syvertsen, and N. Stenseth. 2000. Bush cover and range condition

assessments in relation to landscape and grazing in southern Ethiopia. Landscape ecology **15**:535–546.

Pan, S., and G. Lin. 2012. Invasion traveling wave solutions of a competitive system with dispersal. Boundary Value Problems **2012**:120.

Parizek, B., C. M. Rostagno, and R. Sottini. 2002. Soil erosion as affected by shrub encroachment in northeastern Patagonia. Rangeland Ecology & Management/Journal of Range Management Archives **55**:43–48.

Peng, H.-Y., X.-Y. Li, G.-Y. Li, Z.-H. Zhang, S.-Y. Zhang, L. Li, G.-Q. Zhao, Z.-Y. Jiang, and Y.-J. Ma. 2013. Shrub encroachment with increasing anthropogenic disturbance in the semiarid Inner Mongolian grasslands of China. Catena **109**:39–48.

PICKERING, C. M. 1994. Size-dependent reproduction in Australian alpine Ranunculus. Australian journal of ecology **19**:336–344.

Ratajczak, Z., J. B. Nippert, and S. L. Collins. 2012. Woody encroachment decreases diversity across North American grasslands and savannas. Ecology **93**:697–703.

Raupach, M. 1994. Simplified expressions for vegetation roughness length and zero-plane displacement as functions of canopy height and area index. Boundary-Layer Meteorology **71**:211–216.

Ravi, S., P. D'Odorico, S. L. Collins, and T. E. Huxman. 2009. Can biological invasions induce desertification? The New Phytologist **181**:512–515.

Reed, M., L. Stringer, A. Dougill, J. Perkins, J. Atlhopheng, K. Mulale, and N. Favretto. 2015. Reorienting land degradation towards sustainable land management: Linking sustainable livelihoods with ecosystem services in rangeland systems. Journal of environmental management **151**:472–485.

Roques, K., T. O'connor, and A. R. Watkinson. 2001. Dynamics of shrub encroachment in an African savanna: relative influences of fire, herbivory, rainfall and density dependence. Journal of Applied Ecology **38**:268–280.

Schlesinger, W. H., and A. M. Pilmanis. 1998. Plant-soil interactions in deserts. Biogeochemistry **42**:169–187.

Schlesinger, W. H., J. F. Reynolds, G. L. Cunningham, L. F. Huenneke, W. M. Jarrell, R. A. Virginia, and W. G. Whitford. 1990. Biological feedbacks in global desertification. Science **247**:1043–1048.

Sirami, C., and A. Monadjem. 2012. Changes in bird communities in Swaziland savannas between 1998 and 2008 owing to shrub encroachment. Diversity and Distributions **18**:390–400.

Skarpaas, O., and K. Shea. 2007. Dispersal patterns, dispersal mechanisms, and invasion wave speeds for invasive thistles. The American Naturalist **170**:421–430.

Smith, G. R., H. A. Dingfelder, and D. A. Vaala. 2003. Effect of plant size and density on garlic mustard reproduction. Northeastern Naturalist **10**:269–276.

Sullivan, L. L., B. Li, T. E. Miller, M. G. Neubert, and A. K. Shaw. 2017. Density dependence in demography and dispersal generates fluctuating invasion speeds. Proceedings of the National Academy of Sciences **114**:5053–5058.

Taylor, C. M., and A. Hastings. 2005. Allee effects in biological invasions. Ecology Letters **8**:895–908.

Thompson, S. E., S. Assouline, L. Chen, A. Trahktenbrot, T. Svoray, and G. G. Katul. 2014. Secondary dispersal driven by overland flow in drylands: Review and mechanistic model development. Movement ecology **2**:7.

649 Trollope, W., F. Hobson, J. Danckwerts, and J. Van Niekerk. 1989. Encroachment and
650   control of undesirable plants. Veld management in the Eastern Cape pages 73–89.

651 Turnbull, L., J. Wainwright, and R. E. Brazier. 2010. Changes in hydrology and erosion
652   over a transition from grassland to shrubland. Hydrological Processes: An Interna-
653   tional Journal **24**:393–414.

654 Van Auken, O. 2009. Causes and consequences of woody plant encroachment into western
655   North American grasslands. Journal of environmental management **90**:2931–2942.

656 Van Auken, O. W. 2000. Shrub invasions of North American semiarid grasslands. Annual
657   review of ecology and systematics **31**:197–215.

658 Veit, R. R., and M. A. Lewis. 1996. Dispersal, population growth, and the Allee ef-
659   fect: dynamics of the house finch invasion of eastern North America. The American
660   Naturalist **148**:255–274.

661 Wang, M.-H., M. Kot, and M. G. Neubert. 2002. Integrodifference equations, Allee
662   effects, and invasions. Journal of mathematical biology **44**:150–168.

663 Weiner, J. 1990. Asymmetric competition in plant populations. Trends in ecology &
664   evolution **5**:360–364.

665 Wells, P. V., and J. H. Hunziker. 1976. Origin of the creosote bush (Larrea) deserts of
666   southwestern North America. Annals of the Missouri Botanical Garden pages 843–861.

667 Whitford, W., E. Depree, and P. Johnson. 1980. Foraging ecology of two chihuahuan
668   desert ant species: Novomessor cockerelli andNovomessor albisetosus. Insectes Sociaux
669   **27**:148–156.

670 Whitford, W. G. 1978. Structure and seasonal activity of Chihuahua desert ant commu-
671   nities. Insectes Sociaux **25**:79–88.

672 Wiernga, J. 1993. Representative roughness parameters for homogeneous terrain.

673 Boundary-Layer Meteorology **63**:323–363.